



ELSEVIER

Nuclear Instruments and Methods in Physics Research A 464 (2001) 477–483

**NUCLEAR  
INSTRUMENTS  
& METHODS  
IN PHYSICS  
RESEARCH**  
Section A

www.elsevier.nl/locate/nima

# 3D multispecies nonlinear perturbative particle simulations of collective processes in intense particle beams for heavy ion fusion

Hong Qin\*, Ronald C. Davidson, W. Wei-li Lee, Roman Kolesnikov

*Princeton Plasma Physics Laboratory, Princeton University, Princeton, NJ 08543, USA*

---

## Abstract

Collective processes in intense charged particle beams for heavy ion fusion are studied using a 3D multispecies nonlinear perturbative particle simulation method, which solves self-consistently the nonlinear Vlasov–Maxwell equations. The newly-developed Beam Equilibrium Stability and Transport code is used to simulate the nonlinear stability properties of intense beam propagation, surface and body eigenmodes in a high-intensity beam, and the electron-ion two-stream instability, which occurs when a small population of (unwanted) electrons is present in the system. © 2001 Elsevier Science B.V. All rights reserved.

*Keywords:* Ion beam; Space charge; Stability; Perturbative particle simulation; Collective modes

---

## 1. Introduction

Periodic focusing accelerators and transport systems [1,2] play an important role in heavy ion fusion (see for example [3]). At the high beam currents and charge densities of practical interest for heavy ion fusion, it is increasingly important to develop an improved theoretical understanding of the influence of the intense self fields produced by the beam space charge and current on detailed equilibrium, stability and transport properties. To achieve this goal, it is necessary to study the self-consistent evolution of the beam distribution function  $f_b(\mathbf{x}, \mathbf{p}, t)$  and the self-generated electric and magnetic fields in a kinetic description

[4–7] based on the nonlinear Vlasov–Maxwell equations.

Recently, the  $\delta f$  formalism, a low-noise, nonlinear perturbative particle simulation technique for solving the Vlasov–Maxwell equations, has been developed for intense beam applications, and applied to matched-beam propagation in a periodic focusing field [8,9], and other related studies. The present paper reports recent advances in applying the  $\delta f$  formalism to investigate nonlinear collective processes in intense charged particle beams. The Beam Equilibrium Stability and Transport (BEST) code [10] described here is a newly-developed 3D multispecies nonlinear perturbative particle simulation code, which solves self-consistently the Vlasov–Maxwell equations and can be applied to a wide range of important collective processes in intense beams, such as collective mode excitations [1,11,12], and

---

\*Corresponding author.

*E-mail address:* hongqin@pppl.gov (H. Qin).

periodically-focused beam propagation [7]. The 3D and multispecies capability of the simulation code are required by the physics of the collective processes under investigation. In general, collective processes are nonlinear and have 3D spatial structure, and a second or third species of charged particles is often introduced into the system, either intentionally or unintentionally. For example, when a second background charge species is present, it has been recognized, both in theoretical studies and in experimental observations [13–16], that the relative streaming motion of the high-intensity beam particles through the background charge species provides the free energy to drive the *two-stream* instability, which has a 3D mode structure.

Following a brief description of the nonlinear  $\delta f$  formalism (Section 2), this paper presents detailed simulation results (Section 3) for the nonlinear stability properties of intense beam propagation, surface- and body-mode collective excitations, and the electron–ion two-stream instability, with particular emphasis on the parameter regime characteristic of the high-intensity beams for heavy ion fusion.

## 2. Nonlinear $\delta f$ formalism

The theoretical model employed here that incorporates collective effects is based on the nonlinear Vlasov–Maxwell equations. We consider a thin, continuous, high-intensity ion beam ( $j=b$ ), with characteristic radius  $r_b$  propagating in the  $z$ -direction through background electron and ion components ( $j=e, i$ ), each of which is described by a distribution function  $f_j(\mathbf{x}, \mathbf{p}, t)$  [6,7,13]. The charge components ( $j=b, e, i$ ) propagate in the  $z$ -direction with characteristic axial momentum  $\gamma_j m_j \beta_j c$ , where  $V_j = \beta_j c$  is the average directed axial velocity,  $\gamma_j = (1 - \beta_j^2)^{-1/2}$  is the relativistic mass factor,  $e_j$  and  $m_j$  are the charge and rest mass, respectively, of a  $j$ th species particle, and  $c$  is the speed of light in *vacuo*. While the nonlinear  $\delta f$  formalism outlined here is readily adapted to the case of an applied periodic focusing field, for present purpose we make use of a *smooth-focusing* model in which the applied focusing force is

described by

$$\mathbf{F}_j^{\text{foc}} = -\gamma_j m_j \omega_{\beta j}^2 \mathbf{x}_\perp, \quad (1)$$

where  $\mathbf{x}_\perp = x\hat{\mathbf{e}}_x + y\hat{\mathbf{e}}_y$  is the transverse displacement from the beam axis, and  $\omega_{\beta j} = \text{const}$  is the effective applied betatron frequency for transverse oscillations. Furthermore, in a frame of reference moving with axial velocity  $\beta_j c$ , the motion of a  $j$ th species particle is assumed to be nonrelativistic. The space-charge intensity is allowed to be arbitrarily large, subject only to transverse confinement of the beam ions by the applied focusing force, and the background electrons are confined in the transverse plane by the space-charge potential  $\phi(\mathbf{x}, t)$  produced by the excess ion charge. In the electrostatic and magnetostatic approximations, we represent the self-electric and self-magnetic fields as  $\mathbf{E}^s = -\nabla\phi(\mathbf{x}, t)$  and  $\mathbf{B}^s = \nabla \times [A_z(\mathbf{x}, t)\hat{\mathbf{e}}_z]$ . The nonlinear Vlasov–Maxwell equations in the 6D phase space  $(\mathbf{x}, \mathbf{p})$  can be approximated by [13]

$$\left\{ \frac{\partial}{\partial t} + \mathbf{v} \cdot \frac{\partial}{\partial \mathbf{x}} - \left[ \gamma_j m_j \omega_{\beta j}^2 \mathbf{x}_\perp + e_j \left( \nabla\phi - \frac{v_z}{c} \nabla_\perp A_z \right) \right] \cdot \frac{\partial}{\partial \mathbf{p}} \right\} f_j(\mathbf{x}, \mathbf{p}, t) = 0, \quad (2)$$

and

$$\begin{aligned} \nabla^2 \phi &= -4\pi \sum_j e_j \int d^3 p f_j(\mathbf{x}, \mathbf{p}, t), \\ \nabla^2 A_z &= -\frac{4\pi}{c} \sum_j e_j \int d^3 p v_z f_j(\mathbf{x}, \mathbf{p}, t). \end{aligned} \quad (3)$$

In the nonlinear  $\delta f$  formalism, we divide the total distribution function into two parts,  $f_j = f_{j0} + \delta f_j$ , where  $f_{j0}$  is a *known* equilibrium solution to the nonlinear Vlasov–Maxwell equations (2) and (3), and the numerical simulation is carried out to determine only the detailed nonlinear evolution of the perturbed distribution function  $\delta f_j$ . This is accomplished by advancing the weight function defined by  $w_j \equiv \delta f_j / f_j$ , together with the particles' positions and momenta. The equations of motion for the particles, obtained from the characteristics of the nonlinear Vlasov equation (2), are

given by

$$\begin{aligned}\frac{d\mathbf{x}_{ji}}{dt} &= (\gamma_j m_j)^{-1} \mathbf{p}_{ji}, \\ \frac{d\mathbf{p}_{ji}}{dt} &= -\gamma_j m_j \omega_{\beta j}^2 \mathbf{x}_{\perp ji} - e_j \left( \nabla \phi - \frac{v_{zji}}{c} \nabla_{\perp} A_z \right).\end{aligned}\quad (4)$$

Here the subscript “ $j$ ” labels the  $i$ th simulation particle of the  $j$ th species. The weight functions  $w_j$ , as functions of phase space variables, are carried by the simulation particles, and the dynamical equations for  $w_j$  are easily derived from the definition of  $w_j$  and the nonlinear Vlasov equation (2). Following the algebra in Refs. [8–10], we obtain

$$\begin{aligned}\frac{dw_{ji}}{dt} &= -(1 - w_{ji}) \frac{1}{f_{j0}} \frac{\partial f_{j0}}{\partial \mathbf{p}} \delta \left( \frac{d\mathbf{p}_{ji}}{dt} \right) \\ \delta \left( \frac{d\mathbf{p}_{ji}}{dt} \right) &\equiv -e_j \left( \nabla \delta \phi - \frac{v_{zji}}{c} \nabla_{\perp} \delta A_z \right),\end{aligned}\quad (5)$$

where  $\delta \phi = \phi - \phi_0$  and  $\delta A_z = A_z - A_{z0}$ . Here, the equilibrium solutions  $(\phi_0, A_{z0}, f_{j0})$  solve the steady-state ( $\partial/\partial t = 0$ ) Vlasov–Maxwell equations (2) and (3) with  $\partial/\partial z = 0$  and  $\partial/\partial \theta = 0$ . A wide variety of axisymmetric equilibrium solutions to Eqs. (2) and (3) have been investigated in the literature. The perturbed distribution  $\delta f_j$  is obtained through the weighted Klimontovich representation [1]

$$\delta f_j = \frac{N_j}{N_{sj}} \sum_{i=1}^{N_{sj}} w_{ji} \delta(\mathbf{x} - \mathbf{x}_{ji}) \delta(\mathbf{p} - \mathbf{p}_{ji}), \quad (6)$$

where  $N_j$  is the total number of actual  $j$ th species particles, and  $N_{sj}$  is the total number of *simulation* particles for the  $j$ th species. Maxwell’s equations are also expressed in terms of the perturbed fields and perturbed density according to

$$\nabla^2 \delta \phi = -4\pi \sum_j e_j \delta n_j, \quad \nabla^2 \delta A_z = -\frac{4\pi}{c} \sum_j \delta j_{zj}, \quad (7)$$

where

$$\begin{aligned}\delta n_j &= \int d^3 p \delta f_j(\mathbf{x}, \mathbf{p}, t) = \frac{N_j}{N_{sj}} \sum_{i=1}^{N_{sj}} w_{ji} S(\mathbf{x} - \mathbf{x}_{ji}), \\ \delta j_{zj} &= e_j \int d^3 p v_{zj} \delta f_j(\mathbf{x}, \mathbf{p}, t) \\ &= \frac{e_j N_j}{N_{sj}} \sum_{i=1}^{N_{sj}} v_{zji} w_{ji} S(\mathbf{x} - \mathbf{x}_{ji}).\end{aligned}\quad (8)$$

Here,  $S(\mathbf{x} - \mathbf{x}_{ji})$  represents the method of distributing particles on the grids in configuration space.

The nonlinear particle simulations are carried out by iteratively advancing the particle motions, including the weights they carry, according to Eqs. (4) and (5), and updating the fields by solving the perturbed Maxwell’s equations (7) with appropriate boundary conditions at the cylindrical, perfectly conducting wall. In the longitudinal direction, periodic boundary conditions are used. The equations for  $\delta \phi$  and  $\delta A_z$ , expressed in cylindrical coordinates, are solved using an FFT method in the  $\theta$ - and  $z$ -directions and a finite difference method in the  $r$ -direction. Even though it is a perturbative approach, the  $\delta f$  method is *fully nonlinear* and simulates completely the original nonlinear Vlasov–Maxwell equations. Compared with conventional particle-in-cell simulations, the noise level in  $\delta f$  simulations is significantly reduced. This is because the statistical noise, which is of order  $O(N_s^{-1/2})$  for the total distribution function in the conventional particle-in-cell (PIC) method, is only associated with the perturbed distribution in the  $\delta f$  method. If the same number of simulation particles is used in the two approaches, then the noise level in the  $\delta f$  method is reduced by a factor of  $f/\delta f$  relative to the PIC method. Therefore, to achieve the same accuracy for the perturbed fields, the number of simulation particles used in the  $\delta f$  method is reduced by a factor of  $(f/\delta f)^2$ . Obviously, the noise level in the  $\delta f$  method is comparable to the conventional PIC method, when  $\delta f$  is comparable to  $f$  almost everywhere. However, if this happens over a relatively long period of time, we can adopt a dynamic representation for the equilibrium distribution  $f_{j0}$ , such that  $\delta f$  is always smaller than  $f$ . In addition, the  $\delta f$  method can be used to study *linear* stability properties, provided the factor  $(1 - w_{ji})$  in Eq. (5) is approximated by unity, and the forcing term in Eq. (4) is replaced by the unperturbed force, which is equivalent to integrating along unperturbed particle orbits for the linearized system.

Implementation of the 3D multispecies nonlinear  $\delta f$  simulation method described above is embodied in the BEST code [10] developed at the Princeton Plasma Physics Laboratory. The code

advances the particle motions using a leap-frog method, and solves Maxwell's equations in cylindrical geometry. For those particle motions with much larger characteristic frequency than the frequency of the mode being studied, the code uses an adiabatic field pusher to advance the particles many time steps without solving for the perturbed fields.

### 3. Simulation results

We first present application of the code to a single-species thermal equilibrium ion beam in a constant focusing field. It is assumed that the beam is centered inside a cylindrical chamber with perfectly conducting wall located at  $r=r_w$ , and the equilibrium is 1D, depending only on the radial coordinate  $r=(x^2+y^2)^{1/2}$ . The isotropic thermal equilibrium distribution function in the phase space  $(r, \mathbf{p})$  is given by

$$f_{b0}(r, P) = \frac{\hat{n}_b}{(2\pi\gamma_b m_b T_b)^{3/2}} \times \exp\left\{-\frac{p_\perp^2/2\gamma_b m_b + \gamma_b m_b \omega_{pb}^2 r^2/2 + e_b(\phi_0 - \beta_b A_{z0})}{T_b}\right\} \times \exp\left\{-\frac{(p_z - \gamma_b m_b \beta_b c)^2}{2\gamma_b m_b T_b}\right\}, \quad (9)$$

where  $\hat{n}_b$  is the number density of beam particles at  $r=0$ , and  $T_b = \text{const}$  is the temperature of the beam ions in energy units. The equilibrium self-field potentials  $\phi_0$  and  $A_{z0}$  can be determined numerically from the nonlinear Maxwell's equations in Eq. (3). As an example, we examine the nonlinear propagation properties of a heavy ion beam with  $\gamma_b = 1.08$ , mass number  $A = 133$ , and normalized space-charge intensity  $s_b \equiv \hat{\omega}_{pb}^2/2\gamma_b^2\omega_{\beta b}^2 = 0.95$ . Here,  $\hat{\omega}_{pb}^2 = 4\pi\hat{n}_b e_b^2/\gamma_b m_b$  is the relativistic plasma frequency-squared on axis ( $r=0$ ). A 3D small-amplitude random initial perturbation is introduced into the system, and the beam is propagated from  $t=0$  to  $1200\tau_\beta$ , where  $\tau_\beta \equiv \omega_{\beta b}^{-1}$ . The simulation results show that the perturbations do not grow and the beam propagates quiescently over large distance, which agrees with the nonlinear stability theorem [5] for the choice of monotonically-decreasing equilibrium distribution function in Eq. (9). Shown in Fig. 1

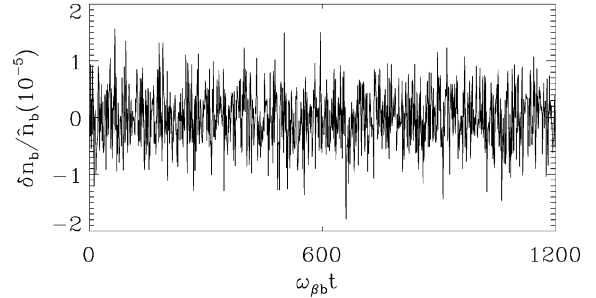


Fig. 1. Time history of  $\delta n_b/\hat{n}_b$  for small-amplitude perturbations about a thermal equilibrium ion beam.

is a plot of the density perturbation at one spatial location versus normalized time  $\omega_{\beta b} t$ , for perturbations about the thermal equilibrium distribution in Eq. (9). The normalized amplitudes of the initial random perturbation in weights in Fig. 1 are of order  $10^{-5}$ , which leads to a very small density perturbation. It is evident from Fig. 1 that the perturbations remain extremely small, and the beam propagates quiescently over very large distances, as expected.

As a second example, we study the linear surface mode for perturbations about a thermal equilibrium ion beam in the space-charge-dominated regime, with flat-top density profile. These modes are of practical interest because they can be destabilized by a two-stream electron–ion interaction when background electrons are present [13–16]. The BEST code, operating in its linear stability mode, has recovered very well-defined eigenmodes with mode structures and eigenfrequencies which agree well with theoretical predications [1,13]. For the dipole mode with azimuthal mode number  $l=1$ , the dispersion relation for these modes is given by [13]

$$\omega = k_z V_b \pm \frac{\hat{\omega}_{pb}}{\sqrt{2\gamma_b}} \sqrt{1 - \frac{r_b^2}{r_w^2}}, \quad (10)$$

where  $r_b$  is the radius of the beam edge, and  $r_w$  is location of the conducting wall. In Eq. (10),  $\hat{\omega}_{pb}^2 = 4\pi\hat{n}_b e_b^2/\gamma_b m_b$  is the ion plasma frequency-squared, and  $\hat{\omega}_{pb}/\sqrt{2\gamma_b} \simeq \omega_{\beta b}$  has been assumed in the space-charge-dominated regime. Shown in Fig. 2 is a comparison between plots of the eigenfrequency

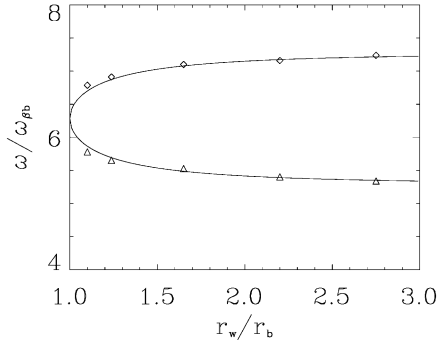


Fig. 2. Plot of the normalized oscillation frequency  $\omega/\omega_{\beta b}$  versus  $r_w/r_b$  for  $l=1$  surface-mode excitations.

versus  $r_w/r_b$  obtained from the simulations (diamonds and triangles) and that predicted by Eq. (10) (solid curves). It is clear from Fig. 2 that the simulation results agree very well with the theoretical predictions.

In addition to the surface modes, there exists a discrete spectrum of collective body-mode oscillations in high-intensity charged particle beams. Here, we study the axisymmetric body modes with  $l=0$  and  $k_z=0$  for perturbations about a moderate-intensity beam with  $s_b \equiv \hat{\omega}_{pb}^2/2\gamma_b^2\omega_{\beta b}^2 = 0.44$ . The system is perturbed at  $t=0$  by an initial density perturbation, which varies smoothly across the beam radius, with zero net perturbed charge density, and normalized amplitude  $10^{-4}$ . In general, discrete eigenmodes can be recovered from the spectrum of the time history of the perturbations. Shown in Fig. 3 is the spectrum of the density perturbation at one spatial location, from which we can clearly identify the first four body eigenmodes of the system at frequencies  $\omega_1 = 1.53\omega_{\beta b}$ ,  $\omega_2 = 2.98\omega_{\beta b}$ ,  $\omega_3 = 4.50\omega_{\beta b}$ , and  $\omega_4 = 6.03\omega_{\beta b}$ . The corresponding potential perturbations,  $\delta\phi_n(r)$ , for each eigenmode are plotted in Fig. 4. We follow the convention in previous analytical and numerical studies [1,11,12], and use the notation  $n=1, 2, 3, \dots$  to label the radial mode number of the discrete eigenmodes. Any (oscillatory) perturbation can be expanded as  $\delta\phi(r, t) = \sum_n a_n \delta\phi_n(r) \exp(-i\omega_n t)$ , where  $a_n$  is the mode amplitude. Numerically,  $\delta\phi_n(r)$  is extracted from  $\delta\phi(r, t)$  by determining the Fourier compo-

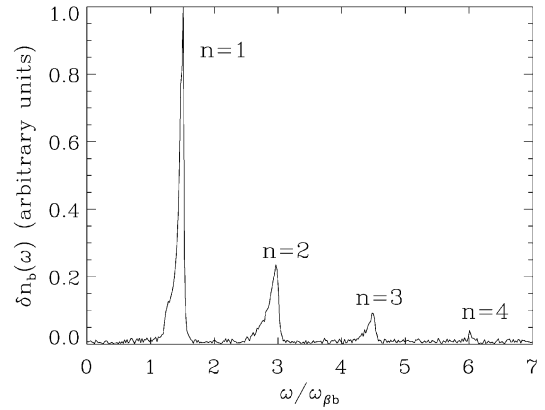


Fig. 3. Frequency spectrum of axisymmetric body eigenmodes.

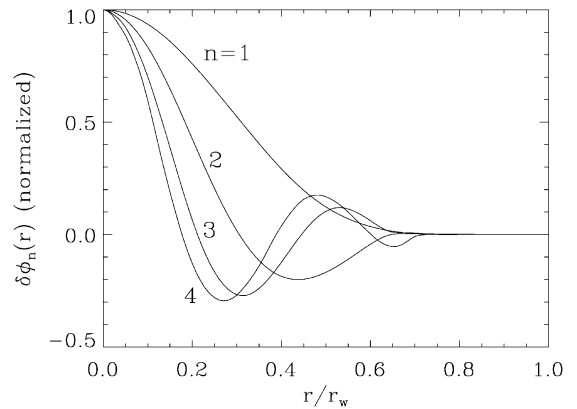


Fig. 4. Radial mode structure of the body eigenmodes in Fig. 3.

nent of  $\delta\phi(r, t)$  oscillating at frequency  $\omega_n$ . As is evident from Fig. 4 and consistent with previous analytical and numerical studies, the eigenfunction  $\delta\phi_n(r)$  has  $n$  zeros when plotted as a function of  $r$ .

The oscillatory eigenmodes studied above are of practical interest because under certain circumstances they can be destabilized by other physical effects. For example, the body modes can be destabilized by pressure anisotropy, when the perpendicular pressure is sufficiently large in comparison with the parallel pressure  $P_{\perp} > P_{\parallel}$  [12,18]. The presence of an unwanted second species of charged particles, such as electrons, can also provide the free energy to drive the system

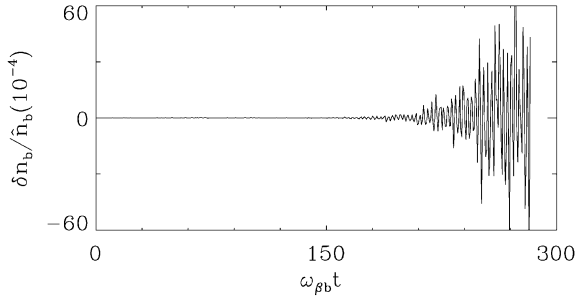


Fig. 5. Electron–ion two-stream instability for illustrative heavy ion fusion parameters.

unstable. The instability observed in the Proton Storage Ring [15,16] is believed to be the electron–proton two-stream instability, and has been simulated using the BEST code [17]. We present here illustrative simulation results for the electron–ion two-stream instability. In the simulations, the equilibrium distribution functions  $f_{j0}(r, \mathbf{p})$  are chosen to be the *bi-Maxwellian* generalizations of Eq. (9), with temperature  $T_{j\perp} = \text{const}$  in the  $x$ – $y$  plane, and temperature  $T_{j\parallel} = \text{const}$  in the  $z$ -direction. Because the two-stream instability is strongest when the beam ions are *cold* in the parallel direction [13] (no Landau damping by parallel kinetic effects), we take  $T_{b\parallel} = 0$  and  $T_{e\parallel} = 0$  in the simulations presented here. The stabilizing influence of longitudinal Landau damping by parallel ion kinetic effects at increasing values of  $T_{b\parallel}/T_{b\perp}$  is reported in Refs. [17,19,20].

Illustrated in Fig. 5 are the initial linear simulation results for the electron–ion two-stream instability for a heavy ion beam ( $A=133$ ,  $Z_b=1$ ) near the space-charge limit, with  $\gamma_b = 1.08$ ,  $f \equiv \hat{n}_e/\hat{n}_b = 0.1 (\omega_{pb}^2/2\omega_{\beta b}^2)(1 - f - \beta_b^2) = 0.994$ ,  $T_{b\perp}/\gamma_b m_b V_b^2 = 4.49 \times 10^{-7}$ ,  $T_{e\perp}/\gamma_b m_b V_b^2 = 7.43 \times 10^{-6}$ ,  $\omega_{\beta e} = 0$ , and  $V_e = 0$  (stationary electrons). The density perturbation amplitude  $\delta n_b$  at one spatial location is plotted versus  $\omega_{\beta b} t$  in Fig. 5 during the linear growth phase of the instability. The simulations show that the most unstable mode is the  $(l, n) = (0, 1)$  body mode, with axial wave-number  $k_z$  and real part of the eigenfrequency  $\omega$  satisfying the resonance conditions  $\omega \simeq \omega_V$  and  $k_z V_b \simeq \omega_e + \omega_b$ , where  $\omega_b$  and  $\omega_e$  are the char-

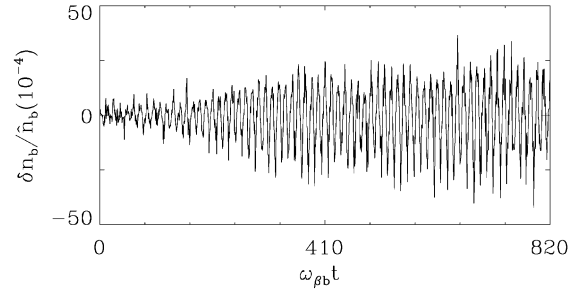


Fig. 6. Linear and nonlinear phases of the electron–proton two-stream instability for illustrative parameters in the Proton Storage Ring experiment.

acteristic collective oscillation frequencies of the beam ions and electrons [1,13]. In this case, the linear growth rate in the simulation is measured to be  $\text{Im } \omega = 0.036 \omega_{\beta b}$ . Shown in Fig. 6 are typical simulation results for the linear and nonlinear phases of the electron–proton two-stream instability in a moderately intense proton beam with  $s_b \equiv \hat{\omega}_{pb}^2/2\gamma_b^2 \omega_{\beta b}^2 = 0.074$ ,  $\gamma_b = 1.85$ ,  $T_{b\perp}/\gamma_b m_b V_b^2 = 3.61 \times 10^{-6}$ ,  $T_{e\perp}/\gamma_b m_b V_b^2 = 5.86 \times 10^{-7}$ ,  $f \equiv \hat{n}_e/\hat{n}_b = 0.1$ ,  $V_e = 0$  and  $\omega_{\beta e} = 0$ . These system parameters correspond to the typical operating parameters in the Proton Storage Ring experiment [15,16]. We see clearly from Fig. 6 the initial linear growth phase and the nonlinear saturation of the instability. For the parameters considered here, the instability nonlinearly saturates at  $t \sim 400 \omega_{\beta b}^{-1}$  at a normalized amplitude of  $\delta n_b / \hat{n}_b \sim 0.3\%$ . Different from the electron–ion two-stream stability for the heavy ion fusion parameters in Fig. 5, the simulations in Fig. 6 indicate that the most unstable mode for the electron–proton two-stream instability is predominantly a surface dipole mode with  $l=1$ .

#### 4. Conclusions

In conclusion, a 3D multispecies nonlinear perturbative particle simulation method has been developed to study collective processes in intense charged particle beams described self-consistently by the Vlasov–Maxwell equations. The simulation

results show that an isotropic thermal equilibrium ion beam in a constant focusing field is nonlinearly stable and can propagate quiescently over hundreds of lattice periods. For the  $l=1$  surface eigenmodes excited in a uniform-density beam, the simulation results agree well with analytical predictions [13]. Axisymmetric body modes have also been studied, and the basic features of these body eigenmodes are in qualitative agreement with previous studies [1,11,12]. Instabilities driven by pressure anisotropy are being investigated using the  $\delta f$  method. Finally, introducing a background component of electrons, strong electron–ion two-stream instabilities are modeled in the simulations. More detailed properties of the electron–ion two-stream instability, such as the nonlinear dynamics and saturation mechanism, are presently under investigation. As a 3D multispecies perturbative particle simulation code, the newly-developed BEST code provides several unique capabilities. Since the simulation particles are used to simulate only the perturbed distribution functions and the perturbed self-fields, the simulation noise is reduced significantly. The perturbative approach also enables the code to investigate different physics effects separately, as well as simultaneously. The code can be easily switched between linear and nonlinear operation, and used to study both linear stability properties and nonlinear beam dynamics. These features, combined with 3D and multispecies capabilities, provide an effective tool to investigate the electron–ion two-stream instability, periodically focused solutions in alternating gradient field configurations, halo formation, and many other important problems in nonlinear beam dynamics and accelerator physics.

### Acknowledgements

This research was supported by the US Department of Energy.

### References

- [1] R.C. Davidson, *Physics of Nonneutral Plasmas*, Addison-Wesley Publishing Co., Reading, MA, 1990, and references therein.
- [2] A.W. Chao, *Physics of Collective Beam Instabilities in High Energy Accelerators*, Wiley, New York, 1993.
- [3] I. Hofmann (Ed.), *Proceedings of the 1997 International Symposium on Heavy Ion Inertial Fusion*, Nucl. Instr. Meth. Phys. Res. A 415 (1988) 1, and references therein.
- [4] R.C. Davidson, *Phys. Plasmas* 5 (1998) 3459.
- [5] R.C. Davidson, *Phys. Rev. Lett.* 81 (1998) 991.
- [6] R.C. Davidson, C. Chen, *Part. Accel.* 59 (1998) 175.
- [7] R.C. Davidson, H. Qin, P.J. Channell, *Phys. Rev. (Special Topics on Accelerators and Beams)* 2 (1999) 074401; 3 (2000) 029901.  
P.J. Channell, *Phys. Plasmas* 6 (1999) 982.
- [8] W.W. Lee, Q. Qian, R.C. Davidson, *Phys. Lett. A* 230 (1997) 347.  
Q. Qian, W.W. Lee, R.C. Davidson, *Phys. Plasmas* 4 (1997) 1915.
- [9] P.H. Stoltz, R.C. Davidson, W.W. Lee, *Phys. Plasmas* 6 (1999) 298.
- [10] H. Qin, R.C. Davidson, W.W. Lee, *Proceedings of the 1999 Particle Accelerator Conference*, Vol. 3, 1999, p. 1626.
- [11] S.M. Lund, Davidson, *Phys. Plasmas* 5 (1998) 3028.
- [12] R.C. Davidson, S. Strasburg, *Phys. Plasmas* 7 (2000) 2657.
- [13] R.C. Davidson, H. Qin, P.H. Stoltz, T.-S. Wang, *Phys. Rev. (Special Topics on Accelerators and Beams)* 2 (1999) 054401, and references therein.
- [14] R.C. Davidson, H. Qin, T.-S. Wang, *Phys. Lett. A* 252 (1999) 213.
- [15] D. Neuffer, E. Colton, D. Fitzgerald, T. Hardek, R. Hutson, R. Macek, M. Plum, H. Thiessen, T.-S. Wang, *Nucl. Instr. Meth. Phys. Res. A* 321 (1992) 1.
- [16] R. Macek, *Proceeding of Workshop on Space Charge Physics in High Intensity Hadron Rings*, American Institute of Physics Conference Proceedings, Vol. 448, 1998, p. 116.
- [17] H. Qin, R.C. Davidson, W.W. Lee, *Phys. Rev. A* 272 (2000) 389.
- [18] S.M. Lund et al., *Proceeding of the 19th International Linac Conference*, Chicago, Illinois, 1998.
- [19] R.C. Davidson, H. Qin, *Phys. Lett. A* 270 (2000) 177.
- [20] R.C. Davidson, H. Qin, I. Kaganovich, W.W. Lee, *Nucl. Instr. and Meth. A* 464 (2001) 493, these proceedings.